Evolution of compact states to molecular ones with coupled channels: The case of the $X(3872)$

Jing Song,[1,2,*] L. R. Dai,[3,2,†] and E. Oset[2,‡]

[1]*School of Physics, Beihang University, Beijing 102206, China*
[2]*Departamento de Física Teórica and IFIC, Centro Mixto Universidad de Valencia-CSIC Institutos de Investigación de Paterna, 46071 Valencia, Spain*
[3]*School of science, Huzhou University, Huzhou, 313000 Zhejiang, China*

(Received 13 July 2023; accepted 20 November 2023; published 14 December 2023)

We study the molecular probability of the $X(3872)$ in the $D^0\bar{D}^{*0}$ and D^+D^{*-} channels in several scenarios. One of them assumes that the state is purely due to a genuine nonmolecular component. However, it gets unavoidably dressed by the meson components to the point that in the limit of zero binding of the $D^0\bar{D}^{*0}$ component becomes purely molecular. Yet, the small but finite binding allows for a nonmolecular state when the bare mass of the genuine state approaches the $D^0\bar{D}^{*0}$ threshold, but, in this case the system develops a small scattering length and a huge effective range for this channel in flagrant disagreement with present values of these magnitudes. Next we discuss the possibility to have hybrid states stemming from the combined effect of a genuine state and a reasonable direct interaction between the meson components, where we find cases in which the scattering length and effective range are still compatible with data, but even then the molecular probability is as big as 95%. Finally, we perform the calculations when the binding stems purely from the direct interaction between the meson-meson components. In summary we conclude, that while present data definitely rule out the possibility of a dominant nonmolecular component, the precise value of the molecular probability requires a more precise determination of the scattering length and effective range of the $D^0\bar{D}^{*0}$ channel, as well as the measurement of these magnitudes for the D^+D^{*-} channel which have not been determined experimentally so far.

DOI: 10.1103/PhysRevD.108.114017

I. INTRODUCTION

The discovery of hadronic states of exotic nature, challenging the standard $q\bar{q}$ nature for mesons and qqq nature for baryons has lead to a revival of hadron physics and many review papers have been devoted to study these new systems [1–10]. One of the recurring questions about such systems is whether they are better explained in terms of compact tetraquarks or pentaquarks, or they follow a different pattern as molecular states of meson-meson for mesonic states or meson-baryon for the baryonic states.

Referring to the last three years (earlier references can be found in the review papers cited), there is a large amount of papers discussing the nature of the states, some claiming a molecular nature of the $D^0\bar{D}^{*0}$ and D^+D^{*-} (and cc) type [11–28], and others claiming a compact tetraquark state [29–33]. Some people advocate a mixture of the two structures [34,35] and discussions around this possible scenario are done in [36,37]. Also much work has been devoted to show the relevance of studying the $X(3872)$ in pp and heavy ion collisions as a means to further learn about the structure of the state [30,38–41]. The possibility of learning about this structure by looking at the $X(3872)$ in a nuclear medium has also been discussed in [42].

As one can see, the majority of papers advocate a molecular structure, but other works find support for the compact tetraquark nature. The fact that the state is so close to the $D^0\bar{D}^{*0}$ threshold favors the molecular structure, and this and other reasons have been used to support the molecular structure. However, as we shall see, the proximity of the state to a threshold does not guarantee by itself that the state is of molecular nature, although certainly is favors it. A discussion on this issue for the $T_{cc}(3875)$ is done in [43].

The purpose of the present work is to shed light on the issue of the $X(3872)$ compositeness. For this purpose we start from a genuine nonmolecular state, which couples to $D^0\bar{D}^{*0}$, a channel where it is observed, and then assume

*Song-Jing@buaa.edu.cn
†dailianrong@zjhu.edu.cn
‡oset@ific.uv.es

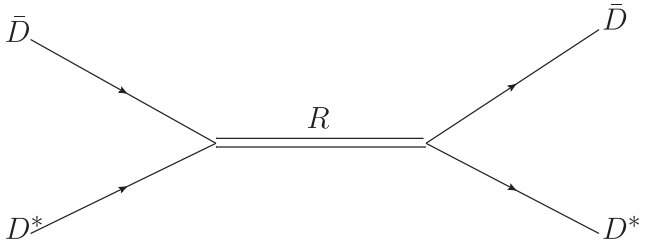

FIG. 1. $D^*\bar{D}$ amplitude from the genuine resonance R.

that by itself it provides a bound state in the $D^0\bar{D}^{*0}$ component. What we observe is that unavoidably the state develops a molecular component and we evaluate its probability, which becomes unity in the limit of zero binding. The question arises about the 'scale' of what small means in the real case and we investigate that in terms of the bare mass of the genuine state. We conclude that it is perfectly possible to have a bound state produced which is still of nonmolecular nature if the genuine state mass is sufficiently close to the threshold. Yet, one pays a price for this, since then, the scattering length of $D^0\bar{D}^0$ becomes small and the effective range grows indefinitely. With present values of this information one can then rule that scenario, concluding the unavoidable molecular nature of the state.

II. FORMALISM

Let us start with a state of nonmolecular nature with a bare mass m_R, which couples to $\bar{D}^0D^{*0}$, D^-D^{*+}. The results of this work come from the mass of these states and we can ignore the complex conjugate component. However, following the isospin assignment of the PDG [44] we will assume that the state has $I=0$ (some isospin breaking will appear as a consequence of the different mass of $\bar{D}^0\bar{D}^{*0}$, D^-D^{*+}). With the isospin multiplets $(D^+,-D^0)$, $(\bar{D}^0,D^-)$, $(D^{*+},-D^{*0})$, $(\bar{D}^{*0},D^{*-})$ the isospin zero state is given by[1]

$$|D^*\bar{D},I=0\rangle=\frac{1}{\sqrt{2}}(D^{*0}\bar{D}^0+D^{*+}D^-). \tag{1}$$

Let us represent the genuine state coupling to this $I=0$ state by

$$t_{D^*\bar{D}}(I=0)=\frac{\tilde{g}^2}{s-s_R} \tag{2}$$

represented by Fig. 1, where s_R represents the mass of this state previous to the unavoidable dressing by the meson-meson component, and $\tilde{g}^2$ provides the strength of this interaction.

From now on we work with the coupled channels $D^{*0}\bar{D}^0$ (1), $D^{*+}D^-(2)$ and the amplitude of Eq. (2) in coupled channels becomes

$$\tilde{V}_R=\begin{pmatrix}\frac{1}{2} & \frac{1}{2}\\ \frac{1}{2} & \frac{1}{2}\end{pmatrix}\frac{\tilde{g}^2}{s-s_R}\equiv\begin{pmatrix}\frac{1}{2}V_R & \frac{1}{2}V_R\\ \frac{1}{2}V_R & \frac{1}{2}V_R\end{pmatrix},\quad \text{with}$$
$$V_R=\frac{\tilde{g}^2}{s-s_R}. \tag{3}$$

The amplitude of Eq. (3) is not unitary. Unitary is accomplished by dressing the amplitude of Fig. 1 with the self-energy of the $\bar{D}D^+$ components, as shown in Fig. 2.

Let T be the unitary amplitude which is given by

$$T=\tilde{V}_R+\tilde{V}_RG\tilde{V}_R+\tilde{V}_RG\tilde{V}_RG\tilde{V}_R+\cdots=\tilde{V}_R+\tilde{V}_RGT \tag{4}$$

with G the diagonal loop matrix

$$G=\begin{pmatrix}G_{D^{*0}\bar{D}^0} & 0\\ 0 & G_{D^{*+}D^-}\end{pmatrix}.$$

The function G is regularized with a cutoff $q_{\max}$, and we find

$$G_i(s)=\int_{|\mathbf{q}|<q_{\max}}\frac{d^3\mathbf{q}}{(2\pi)^3}\frac{w_1^{(i)}+w_2^{(i)}}{2w_1^{(i)}w_2^{(i)}}\times\frac{1}{s-(w_1^{(i)}+w_2^{(i)})^2+i\epsilon}, \tag{5}$$

where $i=D^{*0}\bar{D}^0,D^{*+}D^-$ and w_1, w_2 are given by $w_1=\sqrt{\mathbf{q}^2+m_{D^*}^2}$ $w_2=\sqrt{\mathbf{q}^2+m_{\bar{D}}^2}$. Equation (4) gives

$$T=\left[1-\tilde{V}_RG\right]^{-1}\tilde{V}_R \tag{6}$$

and provides the scattering matrix, T, for the two channels considered. We easily find analytically that

$$T=\frac{1}{\mathrm{DET}}\begin{pmatrix}\frac{1}{2}V_R & \frac{1}{2}V_R\\ \frac{1}{2}V_R & \frac{1}{2}V_R\end{pmatrix}, \tag{7}$$

with DET being the determinant of $(1-\tilde{V}_RG)$

$$\mathrm{DET}=1-\frac{1}{2}V_RG_1-\frac{1}{2}V_RG_2. \tag{8}$$

If we decide to have a bound state at s_0, the T will have a pole at that energy implying

[1]The actual structure in terms of $D^*\bar{D}+cc$ is $\frac{1}{2}(D^{*+}\bar{D}^-+D^{*0}\bar{D}^0-D^{*-}D^+-\bar{D}^{*0}D^0)$, which has $I=0$ and C-parity positive. (We have $CD^{*+}=-D^{*-}$, $CD^+=D^-$, etc.). The couplings of the resonance to Eq. (1) or to the former structure are the same and one can work with the simplified form of Eq. (1).

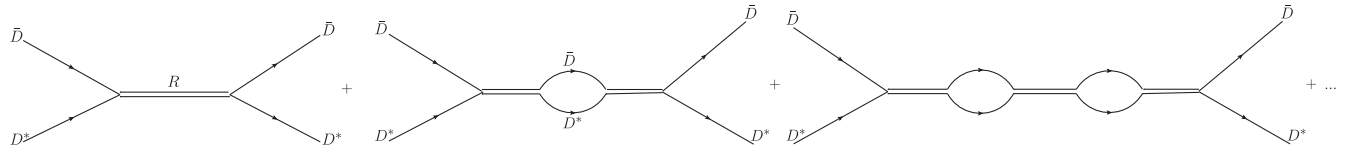

FIG. 2. Dressing of amplitude of Eq. (2) by the $D^*\bar{D}$ self-energy.

$$1-\frac{1}{2}V_R G_1(s_0)-\frac{1}{2}V_R G_2(s_0)=0 \tag{9}$$

from where, given s_R we can obtain $\tilde{g}^2$ as

$$\tilde{g}^2=\left.\frac{s-s_R}{\frac{1}{2}G_1+\frac{1}{2}G_2}\right|_{s_0}. \tag{10}$$

One should note that the $X(3872)$ couples to other channels as $J/\psi\rho$, $J/\psi\omega,\ldots$ [44]. Yet, it is important to differentiate into channels important for the build up of the resonance and those that basically only influence the width of the states. This can be seen for instance in works of vector-vector (VV) interaction, where the VV interaction is responsible for the mass of the state [45,46], and the PP channels (P for pseudoscalar meson) only influence the width of the states from the decay $VV\to PP$ but have a negligible influence in the mass. Another case is the $X_0(2866)$ in the $D^*\bar{K}^*$ picture, where the mass stems from the $D^*\bar{K}^*$ interaction and the $D\bar{K}$ channel is a decay channel which has a negligible influence in the mass of the state [47]. Technically one can envisage it here since the $D^*\bar{D}\to J/\psi\rho$ transition requires the exchange of D of D^*, very suppressed with respect to the exchange of ρ or ω in the $D^*\bar{D}\to D^*\bar{D}$ transition, because of the suppressed D, D^* propagators and the couplings involving three vectors, which are small at threshold.

A. Couplings and probabilities

The couplings to the state for the two channels are given by

$$g_1^2=\lim_{s\to s_0}(s-s_0)T_{11},\qquad g_2^2=\lim_{s\to s_0}(s-s_0)T_{22},$$
$$g_2=g_1\lim_{s\to s_0}(s-s_0)\frac{T_{21}}{T_{11}}. \tag{11}$$

From Eqs. (7) and (8) using L'Hospital's rule we easily find

$$g_1^2=\left.\frac{\frac{1}{2}\tilde{g}^2}{1-\frac{1}{2}\tilde{g}^2\frac{\partial}{\partial s}(G_1+G_2)}\right|_{s_0};\quad g_2=g_1. \tag{12}$$

The fact that $g_2=g_1$ does not exactly imply that we have $I=0$, according to Eq. (1). Indeed, in strong interactions where the isospin manifest itself, given the short range of the interaction, what matters is the wave function at the origin and this is given by [48]

$$\Psi_1(r=0)=g_1G_1(s_0),\qquad \Psi_2(r=0)=g_2G_2(s_0), \tag{13}$$

and, since G_1 and G_2 are different due to the different mass of the channels, Ψ_1 and Ψ_2 are a bit different. The discussion about isospin violation for the $X(3872)$ was already done in Ref. [49].

Once we have the couplings g_1^2 and g_2^2, we can calculate the probabilities to have the $D^{*0}\bar{D}^0$ and $D^{*+}D^-$ in the wave function of the $X(3872)$ as [48,50]

$$P_1=-g_1^2\left.\frac{\partial G_1}{\partial s}\right|_{s_0}=-\left.\frac{\frac{1}{2}\tilde{g}^2\frac{\partial G_1}{\partial s}}{1-\frac{1}{2}\tilde{g}^2\frac{\partial}{\partial s}(G_1+G_2)}\right|_{s_0},$$
$$P_2=-g_2^2\left.\frac{\partial G_2}{\partial s}\right|_{s_0}=-\left.\frac{\frac{1}{2}\tilde{g}^2\frac{\partial G_2}{\partial s}}{1-\frac{1}{2}\tilde{g}^2\frac{\partial}{\partial s}(G_1+G_2)}\right|_{s_0}. \tag{14}$$

Since the $X(3872)$ is closer to the channel 1 threshold ($D^{*0}\bar{D}^0$) and $\frac{\partial G_1}{\partial s}\to\infty$ when $s_0\to s_{\rm th1}$ we immediately find that:

(1) When $\tilde{g}^2\to 0$, $P_1\to 0$, $P_2\to 0$, genuine state;
(2) When $\tilde{g}^2\to\infty$, $P_1+P_2=1$, completely molecular;
(3) When $s_0\to s_{\rm th1}$, $\frac{\partial G_1}{\partial s}\to\infty$, and $\frac{\partial G_2}{\partial s}\to$ finite, $P_1\to 1$, $P_2\to 0$, completely molecular state dominated by the $D^{*0}\bar{D}^0$ component.

Let us stress again that even if $P_1\to 1$, $P_2\to 0$, in strong interaction of zero range what matters is the wave function at the origin and the $D^{*0}\bar{D}^0$ and $D^{*+}D^-$ components become equally important [49].

B. Inclusion of direct interaction between channels

As shown in [48] and the different pictures claiming a molecular nature for the $X(3872)$, there is a direct interaction between the $D^*\bar{D}$ components due to meson exchange. There are differences between the different models but all them conclude that the interaction is attractive. In the local hidden gauge approach the interaction comes from the exchange of vector mesons [51–54]. The vertices needed for this interaction can be obtained from the Lagrangian

$$\mathcal{L}=-ig'\langle[P,\partial_\mu P]V^\mu\rangle, \tag{15}$$

with $g'=\frac{m_{\rm v}}{2f_\pi}$, $m_{\rm v}=800$ MeV, $f_\pi=93$ MeV, where P, V are the $q\bar{q}$ matrices expressed in terms of pseudoscalars, vector mesons [55] and $\langle\rangle$ is the trace of the matrices.

In addition we also need the VVV couplings which are given by the Lagrangian

$$\mathcal{L} = ig'\langle (V_\mu \partial_\nu V^\mu - \partial_\nu V_\mu V^\mu) V^\nu \rangle. \tag{16}$$

With these two couplings one evaluates the transition potentials $VP \to VP$ through the exchange of vector mesons. There is also the possibility to have $VP \to PV \to VP$ which involves twice the VPP Lagrangian of Eq. (1) when one has the transition $VP \to PV$ via P exchange, but with the three momentum part of the vertex. However, these transitions are highly suppressed compared to light vector exchange in $VP \to VP$, as described in detail on Ref. [56] (Appendix B). Actually, in the same work (Appendix A) it is shown that the exchange of vector mesons leads to the chiral Lagrangians in $SU(3)$ derived from chiral symmetry arguments in Ref. [57]. Note that the $VP \to VP$ via P exchange, which would involve the allowed VVP vertex, is forbidden by the extra PPP vertex needed in the evaluation.

With the exchange of ρ, w mesons we obtain an interaction

$$\tilde{V} = \begin{pmatrix} \frac{1}{2}V & \frac{1}{2}V \\ \frac{1}{2}V & \frac{1}{2}V \end{pmatrix} \tag{17}$$

with

$$\frac{1}{2}V = -g'^2 \frac{4 m_{D^{*0}} m_{D^0}}{m_V^2}, \tag{18}$$

calculated at the threshold. We use this interaction as a scale of the interaction, keeping in mind that the binding is tied to the interaction but also to $q_{\max}$ in the G function of Eq. (5) [in one channel one has $T = (V^{-1} - G)^{-1}$ and the pole appears at $V^{-1} - G = 0$, hence, changes of V^{-1} can be accommodated by changes in $q_{\max}$ and vice versa. We shall play with this flexibility by showing results with two different values of $q_{\max}$]. The formulas obtained before for $\tilde{g}^2$, the couplings and probabilities are trivially modified by changing

$$V_R \to V_R + \beta V, \tag{19}$$

where β, for the sake of showing which is the result of adding a direct interaction, will be taken for each $q_{\max}$ such that we barely do not bind the state with only the βV interaction, in other words we would get the binding energy zero with this value of β for the chosen value of $q_{\max}$.

C. Scattering length and effective range

With the normalization of G in Eq. (5) and our choice of V_R and V, we have the relationship between our T matrix and the scattering matrix used in quantum mechanics as

$$T = (-8\pi\sqrt{s}) f^{QM} \simeq (-8\pi\sqrt{s}) \frac{1}{-\frac{1}{a} + \frac{1}{2} r_0 k^2 - ik} \tag{20}$$

with a and r_0 the scattering length and effective range. We have these magnitudes defined for every channel from T_{11} and T_{22}. Then we easily find

$$T_{jj} = \frac{1}{\frac{s - s_R}{\frac{1}{2}[\tilde{g}^2 + \beta V(s - s_R)]} - G_1 - G_2}, \qquad j = 1, 2 \tag{21}$$

where

$$\begin{aligned} &-\frac{1}{a} + \frac{1}{2} r_0 k^2 - ik \\ &= (-8\pi\sqrt{s})(T_{jj})^{-1} \\ &= (-8\pi\sqrt{s}) \left\{ \frac{s - s_R}{\frac{1}{2}[\tilde{g}^2 + \beta V(s - s_R)]} - G_1 - G_2 \right\}. \end{aligned} \tag{22}$$

We immediately see that $-ik$ for the two channels comes automatically from $i 8\pi\sqrt{s} \mathrm{Im} G_j$ since $\mathrm{Im} G = \frac{-1}{8\pi\sqrt{s}} k$. Then we obtain

$$-\frac{1}{a_1} = (-8\pi\sqrt{s}) \left[\frac{s - s_R}{\frac{1}{2}[\tilde{g}^2 + \beta V(s - s_R)]} - \mathrm{Re} G_1 - G_2 \right] \Bigg|_{s_{\mathrm{th1}}}, \tag{23}$$

$$r_{0,1} = 2 \frac{\sqrt{s}}{\mu_1} \frac{\partial}{\partial s} \left\{ (-8\pi\sqrt{s}) \left[\frac{s - s_R}{\frac{1}{2}[\tilde{g}^2 + \beta V(s - s_R)]} - \mathrm{Re} G_1 - G_2 \right] \right\} \Bigg|_{s_{\mathrm{th1}}}, \tag{24}$$

$$-\frac{1}{a_2} = (-8\pi\sqrt{s}) \left[\frac{s - s_R}{\frac{1}{2}[\tilde{g}^2 + \beta V(s - s_R)]} - \mathrm{Re} G_2 - G_1 \right] \Bigg|_{s_{\mathrm{th2}}}, \tag{25}$$

$$r_{0,2} = 2 \frac{\sqrt{s}}{\mu_2} \frac{\partial}{\partial s} \left\{ (-8\pi\sqrt{s}) \left[\frac{s - s_R}{\frac{1}{2}[\tilde{g}^2 + \beta V(s - s_R)]} - \mathrm{Re} G_2 - G_1 \right] \right\} \Bigg|_{s_{\mathrm{th2}}}, \tag{26}$$

with μ_i the reduced mass of the channel.

Note that in Eqs. (23) and (24) G_2 is real. However, in Eqs. (25) and (26) G_1 is complex since it is evaluated at the second threshold $s_{\mathrm{th2}} > s_{\mathrm{th1}}$. Then a_2 and $r_{0,2}$ will be complex, while a_1 and $r_{0,1}$ will be real in the approximation that we do of neglecting the D^* width. The changes introducing the D^* width are small as seen in the study of the $T_{cc}(3875)$ [58], definitely much smaller than the differences that we find for different scenarios of the structure of the $X(3872)$.

The formulas in Eqs. (23)–(26) can equally be used for the case neglecting the direct interaction between the components, simply setting $\beta = 0$.

III. RESULTS

We take the masses from the PDG as

$$m_{D^{*0}} = 2006.85\ \text{MeV}, \quad m_{D^0} = 1864.84\ \text{MeV}, \quad m_{D^{*+}} = 2010.26\ \text{MeV}, \quad m_{D^+} = 1869.66\ \text{MeV},$$
$$m_{X(3872)} = 3871.65\ \text{MeV}, \quad m_{D^{*0}} + m_{D^0} = 3871.69\ \text{MeV}, \quad m_{D^{*+}} + m_{D^-} = 3879.92\ \text{MeV}, \tag{27}$$

and as we can see, the $X(3872)$ state is barely 40 KeV below the $D^{*0}\bar{D}^0$ threshold and is extremely weakly bound. We take different values of $\sqrt{s_R} = \sqrt{s}_{\text{th1}} + \Delta\sqrt{s_R}$ and plot the results for different values of $\Delta\sqrt{s_R}$.

In Figs. 3–6 we neglect the direct interaction of the mesons, ($\beta = 0$) in Eq. (19). In Fig. 3 left we see the results for P_1 and P_2 for $\Delta\sqrt{s_R} = 100$ MeV, meaning that the mass of the genuine state is 100 MeV above the $D^{*0}\bar{D}^0$ threshold. What we observe is that as $\sqrt{s_0}$ goes to the $D^{*0}\bar{D}^0$ threshold, P_1 goes to 1 and P_2 goes to zero, as we expected. We also see that at the energy of $X(3872)$ the probability $P_1 \sim 0.9$ and $P_2 \sim 0.05$ depending a bit on the choice of q_{max}. In Fig. 3 right we show $P_1 + P_2$ to see the convergence to 1 of the sum of the two components when we approach s_{th1}. The total molecular probability is around 0.95 at the $X(3872)$ energy. This means that we started from a state that was purely nonmolecular but it got dressed by the meson-meson component to the point that this component assumes most of the probability in the wave function of the state.

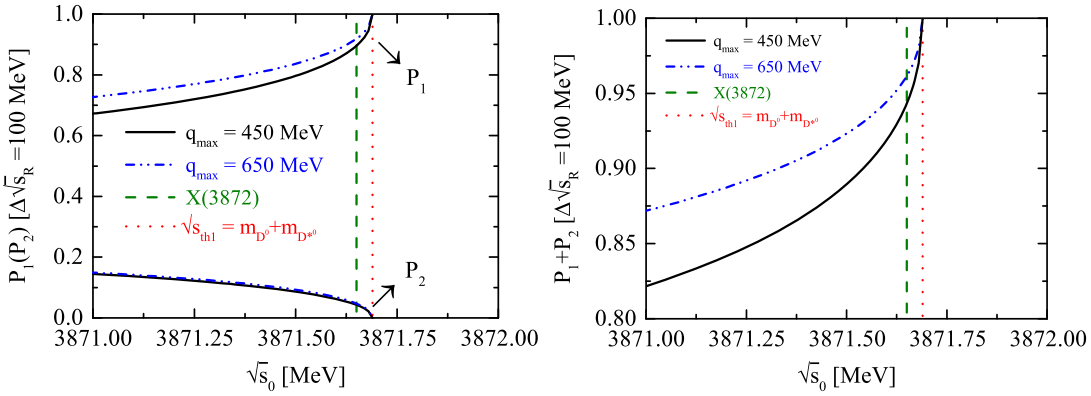

FIG. 3. The evolution of P with $\sqrt{s}$ by taking $\Delta\sqrt{s_R} = 100$ MeV and $\beta = 0$ (no meson-meson interaction). The red lines are the threshold of D^0D^{*0}, the olive-dashed lines are the bound state of $X(3872)$, and the black and blue curves present the behaviors of $q_{\text{max}} = 450$ MeV and $q_{\text{max}} = 650$ MeV, respectively.

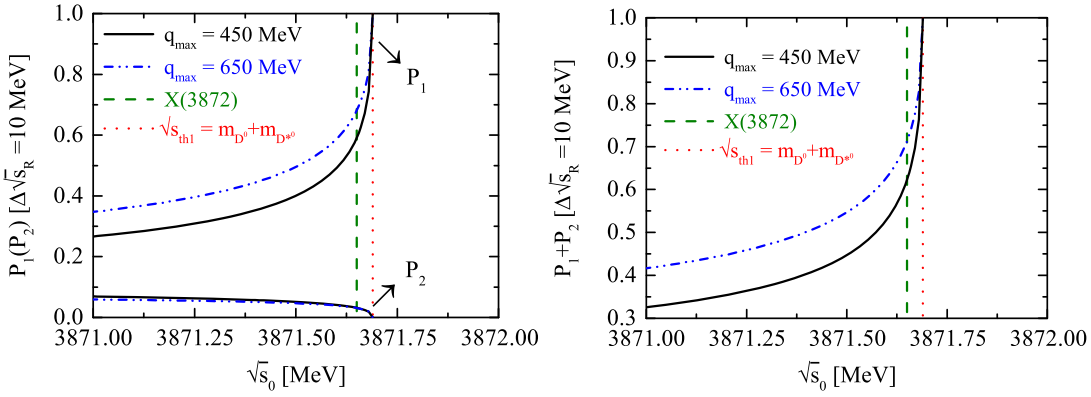

FIG. 4. The labels are same as Fig. 3. Results for $\Delta\sqrt{s_R} = 10$ MeV and $\beta = 0$ (no meson-meson interaction).

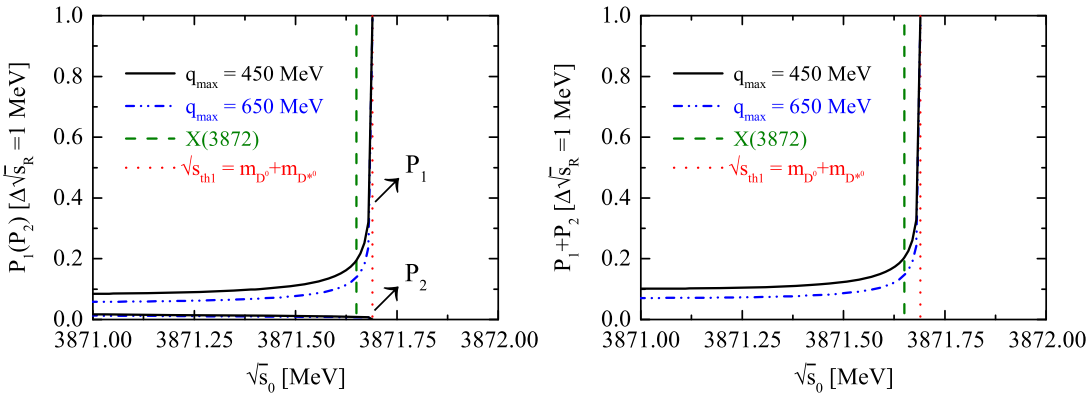

FIG. 5. The labels are same as Fig. 3. Results for $\Delta\sqrt{s_R} = 1$ MeV and $\beta = 0$ (no meson-meson interaction).

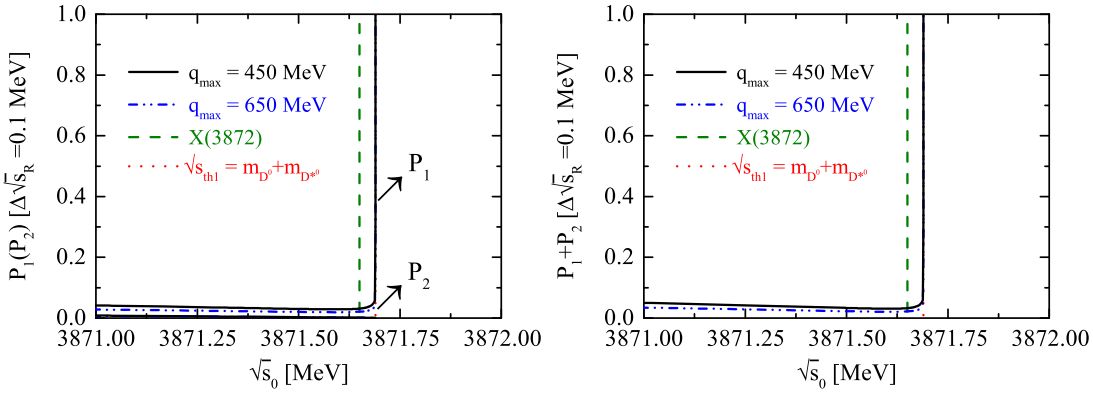

FIG. 6. The labels are same as Fig. 3. Results for $\Delta\sqrt{s_R} = 0.1$ MeV and $\beta = 0$ (no meson-meson interaction).

In Fig. 4 (left) we repeat the procedure with a m_R mass closer to the $D^{*0}\bar{D}^0$ threshold, only 10 MeV above. We observe that the theorem of $P_1 \to 1$ at threshold holds again, but at the pole of the $X(3872)$ $P_1 \sim 0.6$–0.7 and $P_2 \approx 0.03$. In Fig. 4 (right) we see that $P_1 + P_2 \sim 0.6$–0.7. In this case the molecular probability is smaller than before, indicating that if the bare mass of the genuine state is closer to threshold the amount of induced molecular component is smaller, but still sizeable.

In Fig. 5 (left) we repeat the procedure with $\Delta\sqrt{s_R} =$ 1 MeV. In this case at $\sqrt{s_0}$ the value of $P_1 \sim 0.15$–0.2 and the one of $P_2 \approx 0.01$. The sum $P_1 + P_2$ is shown in Fig. 5 right and we see that $P_1 + P_2 \sim 0.15$–0.2, very small.

Finally in Fig. 6 we show the results for $\Delta\sqrt{s_R} =$ 0.1 MeV. In this case we see that the $P_1 + P_2$ is around 0.02, indicating that the induced molecular component is negligible.

The conclusion from all these results is that the binding energy by itself does not give us the molecular probability and it is possible to have a very small binding and still have a negligible molecular component.

However, we can see what happens with a and r_0 in those cases. This is shown in Table I. What we can see is that the scattering lengths a_1, a_2 become small, and most important, the values of the effective range become extremely large, bigger than 600 fm in size for the case of $\Delta\sqrt{s_R} = 0.1$ MeV when we had a negligible molecular component. This should be contrasted with present experimental values. From the study of the line shape in $D\bar{D}\pi$ production of LHCb [59] the authors of Ref. [30] induce

$$r_{0,1} = -5.34 \text{ fm}. \tag{28}$$

However, the authors of [60] redo an analysis of the data and after subtracting the contribution from the second channel they get a value of around -3.78 fm. Different corrections from unknown elements in the theoretical framework reduce the radius $r_{0,1}$ to [61]

$$-2.78 \text{ fm} < r_{0,1} < 1 \text{ fm}. \tag{29}$$

The value extracted for a_1, after accounting for the different prescription in [60] ($\frac{1}{a}$ instead of $-\frac{1}{a}$ in our case), is

$$a_1 \approx 28 \text{ fm}, \tag{30}$$

and has large uncertainties due to uncertainties in the binding.

TABLE I. The value of scattering length a and r_0 at threshold for different $q_{\max}$ and different values of $\Delta\sqrt{s_R}$. $\beta = 0$ in this case (no meson-meson interaction).

	$q_{\max} = 450$ MeV				$q_{\max} = 650$ MeV			
$\Delta\sqrt{s_R}$ (MeV)	a_1 (fm)	$r_{0,1}$ (fm)	a_2 (fm)	$r_{0,2}$ (fm)	a_1 (fm)	$r_{0,1}$ (fm)	a_2 (fm)	$r_{0,2}$ (fm)
0.1	1.42	−663.61	$0.0073 - i0.00003$	$-664.79 - i1.56$	0.954	−1011.3	$0.0048 - i0.00002$	$-1014.0 - i1.56$
0.3	3.16	−273.51	$0.0176 - i0.00020$	$-273.04 - i1.56$	2.181	−416.86	$0.0116 - i0.00009$	$-417.03 - i1.56$
1	7.48	−89.71	$0.0530 - i0.00180$	$-88.46 - i1.56$	5.544	−136.78	$0.0350 - i0.00078$	$-135.77 - i1.56$
2	11.09	−45.95	$0.1014 - i0.00660$	$-44.52 - i1.56$	8.760	−70.098	$0.0674 - i0.00292$	$-68.81 - i1.56$
5	15.80	−18.86	$0.2305 - i0.03475$	$-17.31 - i1.56$	13.67	−28.816	$0.1571 - i0.01597$	$-27.35 - i1.56$
10	18.45	−9.68	$0.3957 - i0.10756$	$-8.10 - i1.56$	16.87	−14.837	$0.2827 - i0.05290$	$-13.31 - i1.56$
20	20.16	−5.07	$0.5902 - i0.26910$	$-3.47 - i1.56$	19.11	−7.8049	$0.4593 - i0.14915$	$-6.25 - i1.56$
50	21.35	−2.29	$0.7558 - i0.58190$	$-0.68 - i1.56$	20.79	−3.5725	$0.6801 - i0.39616$	$-2.00 - i1.56$
70	21.59	−1.76	$0.7761 - i0.68790$	$-0.15 - i1.56$	21.14	−2.7652	$0.7296 - i0.50085$	$-1.19 - i1.56$
100	21.78	−1.37	$0.7818 - i0.78157$	$0.25 - i1.56$	21.41	−2.1595	$0.7611 - i0.60330$	$-0.58 - i1.56$

The discrepancy of the results in Table I, when one has a small molecular component, with the experimental data on a_1 and $r_{0,1}$ is large, enough to discard this scenario. The values obtained for these magnitudes for $\sqrt{s_R} = 100$ MeV, would be basically acceptable, but in this case we found that the molecular component is close to unity.

A. Results with a mixture of genuine state and direct meson-meson interaction

As mentioned before, we conduct now another test in which, in addition to the genuine state, we add the direct interaction between the mesons with a strength that does not bind by itself. The strength of this interaction is chosen from the local hidden gauge potential, gauged by a factor such that the state would be bound with zero energy. As mentioned above, the strength of the potential and the regulator of the loop function G of Eq. (5) are intimately related. We accomplish the previous task by multiplying Eq. (18) by $\beta = 0.320$ for $q_{\max} = 650$ MeV and $\beta = 0.485$ for $q_{\max} = 450$ MeV. These values of $q_{\max}$ are in line with the value 420 MeV demanded to get the experimental binding of the $T_{cc}(3875)$ [62]. The results can be seen in Figs. 7 and 8. If we look now at Fig. 7, we see that for $\Delta\sqrt{s_R} = 100$ MeV $P_1 + P_2$ at the pole is around 1, most of it coming from the $D^{*0}\bar{D}^0$ channel. We should note that this number went up from 0.95 in Fig. 3 in the absence of any direct meson-meson interaction. In Fig. 8, we show the results for $\Delta\sqrt{s_R} = 1$ MeV. We see that $P_1 + P_2$ at the pole is about 0.95. But this number went up from 0.15–0.2 in Fig. 5 in the absence of direct meson-meson interaction. It is clear that as soon as the extra meson-meson interaction is considered, the state becomes essentially molecular.

As we can see, the presence of a reasonable direct meson-meson interaction has as a consequence a drastic increase in the molecular probability of the state.

Next we show in Table II the results that we obtain for a and r_0 in this scenario. Comparing these results with those in Table I, we see that the consideration of the direct meson interaction has also a drastic effect in the increase of the scattering length and the decrease of the size of r_0. While for values of $\Delta\sqrt{s_R}$ of about 0.1 MeV the value of a_1 and $r_{0,1}$ are still unacceptable. for $\Delta\sqrt{s_R} = 1$ MeV, they can be acceptable with the current uncertainty in the experimental values. The discrepancy of a with the value of 21.38 fm with the value of Eq. (30) is not significant in view of the

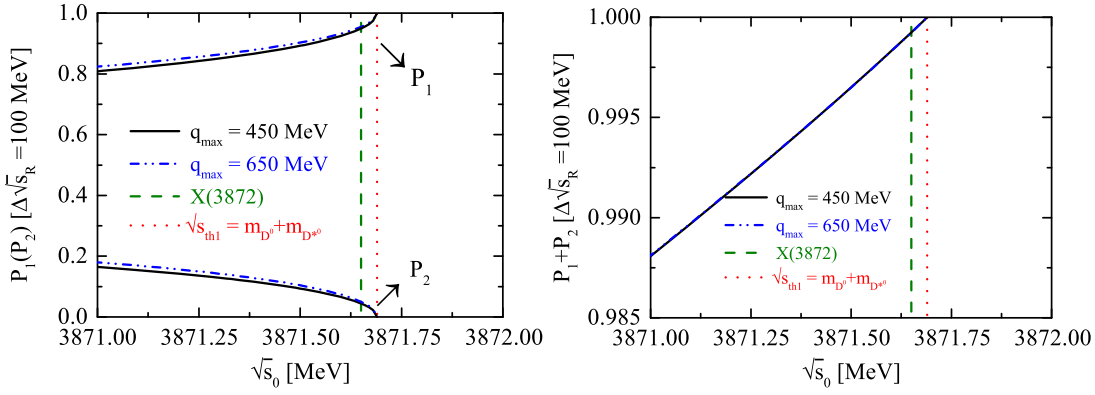

FIG. 7. The labels are same as Fig. 3. Results for the mixture of genuine state and direct meson-meson interaction, with $\Delta\sqrt{s_R} = 100$ MeV. $\beta = 0.320$ for $q_{\max} = 650$ MeV and $\beta = 0.485$ for $q_{\max} = 450$ MeV.

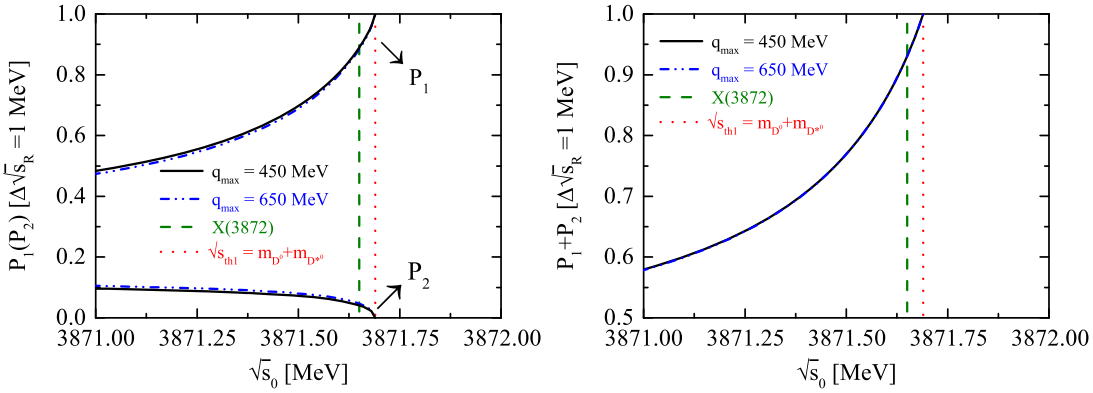

FIG. 8. The labels are same as Fig. 3. Results for the mixture of genuine state and direct meson-meson interaction, with $\Delta\sqrt{s_R} = 1$ MeV. $\beta = 0.320$ for $q_{\max} = 650$ MeV and $\beta = 0.485$ for $q_{\max} = 450$ MeV.

present uncertainties in the binding of the $X(3872)$. However, we saw before that $P_1 + P_2 \sim 0.95$ in this case. This means that at present, a mixed scenario with direct meson-meson interaction and a genuine state, with molecular probabilities around 0.95 can not be discarded. This scenario would be close to the one advocated in [35]. Yet, this is tied to the possible existence of a genuine state that prior to the dressing with the pion cloud has a mass extremely close to threshold, something that is not the case in ordinary tetraquark calculations. In order to see the differences with the scenario in which the state is purely molecular, generated exclusively from the meson-meson interaction we conduct a final test in the next subsection.

B. Results from direct meson-meson interaction alone

Now we demand that the $X(3872)$ is obtained from the meson-meson interaction without any contributions of the genuine state. This is accomplished by taking $\tilde{g}^2 = 0$ and gauging to interaction of Eq. (18) with the factor β. This is accomplished by taking $\beta = 0.324$ for $q_{\max} = 650$ MeV and $\beta = 0.494$ for $q_{\max} = 450$ MeV (the value β would be $\beta = 0.537$ for $q_{\max} = 420$ MeV used in [62]). In this case the state is purely molecular [48], $P_1 + P_2 = 1$, and we show in Table III the results for a and r_0. We can see that these values are very similar for any of the two values of $q_{\max}$ used once we demand to obtain the bound state at the right energy. The small differences give us a idea of the theoretical uncertainties that we can expect. The value for $a_1 = 22$ fm is in line with the one of Eq. (30) in view of the experimental uncertainties in the binding energy. It is also very similar to the value of a_1 obtained in Table II for $\Delta\sqrt{s_R} = 1$ MeV when using the mixture of genuine state and direct meson-meson interaction. The radius $r_{0,1}$ is appreciably different $\sim 0.5 - (-)0.8$ fm versus -2.30 fm. It is thus clear that an improvement in the measured value of $r_{0,1}$ can shed further light on the issue. On the other hand, there is extra information from a_2 and $r_{0,2}$. Curiously, these values in Table III are very similar to those in Table II for $\Delta\sqrt{s_R} = 1$ MeV, indicating that the crucial measurements are those of a_1 and $r_{0,1}$, particularly the second. However, we should note that the values of Table III for a_2 and $r_{0,2}$ are drastically different from those of Table I in the case of only the genuine state for small values of $\Delta\sqrt{s_R}$ where we would have chances of a small molecular component. All this is

TABLE II. The value of scattering length a and r_0 at threshold for different $q_{\max}$ and different values of $\Delta\sqrt{s_R}$ for the mixture of genuine state and direct meson-meson interaction. $\beta = 0.320$ for $q_{\max} = 650$ MeV and $\beta = 0.485$ for $q_{\max} = 450$ MeV.

	$q_{\max} = 450$ MeV				$q_{\max} = 650$ MeV			
$\Delta\sqrt{s_R}$ (MeV)	a_1 (fm)	$r_{0,1}$ (fm)	a_2 (fm)	$r_{0,2}$ (fm)	a_1 (fm)	$r_{0,1}$ (fm)	a_2 (fm)	$r_{0,2}$ (fm)
0.1	15.60	−24.97	$0.7068 - i1.116$	$1.17 - i1.56$	15.84	−25.74	$0.7476 - i1.011$	$0.82 - i1.56$
0.3	19.65	−7.13	$0.7060 - i1.118$	$1.16 - i1.56$	19.50	−7.55	$0.7470 - i1.012$	$0.81 - i1.56$
1	21.38	−2.30	$0.7024 - i1.125$	$1.14 - i1.56$	21.23	−2.64	$0.7448 - i1.019$	$0.78 - i1.56$
2	21.79	−1.35	$0.6957 - i1.139$	$1.08 - i1.56$	21.64	−1.68	$0.7406 - i1.032$	$0.72 - i1.56$
5	22.05	−0.81	$0.6394 - i1.232$	$0.23 - i1.56$	21.90	−1.13	$0.7035 - i1.128$	$-0.11 - i1.56$
10	22.13	−0.63	$0.7818 - i0.780$	$-3.62 - i1.56$	21.98	−0.94	$0.7767 - i0.693$	$-4.32 - i1.56$
20	22.17	−0.54	$0.7514 - i0.998$	$0.92 - i1.56$	22.02	−0.85	$0.7731 - i0.898$	$0.56 - i1.56$
50	22.20	−0.48	$0.7410 - i1.031$	$1.12 - i1.56$	22.05	−0.80	$0.7677 - i0.930$	$0.77 - i1.56$
70	22.21	−0.47	$0.7396 - i1.035$	$1.14 - i1.56$	22.05	−0.79	$0.7669 - i0.934$	$0.79 - i1.56$
100	22.21	−0.47	$0.7385 - i1.038$	$1.15 - i1.56$	22.06	−0.78	$0.7663 - i0.937$	$0.80 - i1.56$

TABLE III. The value of scattering length a and r_0 at threshold for different $q_{\max}$ in the case of only meson-meson interaction. $\beta = 0.324$ for $q_{\max} = 650$ MeV, and $\beta = 0.494$ for $q_{\max} = 450$ MeV.

$q_{\max}$ (MeV)	a_1 (fm)	$r_{0,1}$ (fm)	a_2 (fm)	$r_{0,2}$ (fm)
450	22.22	−0.449	$0.736 - i1.04$	$1.17 - i1.56$
650	22.07	−0.763	$0.765 - i0.94$	$0.82 - i1.56$

telling us that the precise values of $a_2, r_{0,2}, a_2$, and $r_{0,2}$ are crucial to pin down the precise nature of the $X(3872)$. In this sense it is worth mentioning that this information is available for the $T_{cc}(3875)$ [63–65] and it was used in [58] to conclude that the $T_{cc}(3875)$ was purely molecular, with an uncertainty of the order of 2%. In this direction, there has been a recent revival concerning the relevance of a and r_0 to determine the compositeness of states [66,67] improving on the Weinberg prescription [68], considering explicitly the range of the interaction. Definitely, the knowledge of a and r_0 for two coupled channels allows one to be more predictive as proved in the case of $T_{cc}(3875)$ in [58]. We look forward to having these magnitudes measured with precision to give a definite answer to the problem.

C. Couplings in the different scenarios

It is interesting to present the values for the couplings of $\tilde{g}$ and g_1, g_2. We show some sample cases. In Table IV we present the results for $q_{\max} = 450$ MeV and $q_{\max} = 650$ MeV and two different values of $\Delta\sqrt{s}_R$. The value of $\tilde{g}$ changes much with $\Delta\sqrt{s}_R$. For the small value of 0.1 MeV where the state is basically nonmolecular the value of $\tilde{g}$ is small. For $\Delta\sqrt{s}_R = 5$ MeV, $\tilde{g}$ becomes bigger and so do the couplings $g_1 = g_2$, indicating that the state becomes more molecular.

In Table V we consider the pure molecular case, where the state appears as a consequence of the meson-meson interaction. According to the conclusions of the paper, these should be the realistic couplings of the $X(3872)$ to the meson-meson components. It is interesting to remark that these results are very close to those obtained with the simple formula for molecular bound states of Eq. (59) of Ref. [48]

$$g = E_\alpha (16\pi\gamma/\mu)^{1/2} \tag{31}$$

with $\gamma = \sqrt{2\mu B}$, E_α the mass of the state and μ the reduced mass of D^0 and D^{*0}.

TABLE IV. Values of $\tilde{g}$ and g_1, g_2 for the bound state at 3871.65 MeV, with different $q_{\max}$ corresponding to Table I, with no meson-meson interaction, $\beta = 0$.

	$q_{\max} = 450$ MeV		$q_{\max} = 650$ MeV	
$\Delta\sqrt{s}_R$ (MeV)	$\tilde{g}$	$g_1 = g_2$	$\tilde{g}$	$g_1 = g_2$
0.1	681.10	473.51	551.75	385.74
5	4087.89	1929.96	3311.55	1732.38

TABLE V. Values of g_1, g_2, for the molecular case, with only the meson-meson interaction. $\tilde{g} = 0$, corresponding to Table III.

	$q_{\max} = 450$ MeV	$q_{\max} = 650$ MeV
$g_1 = g_2$	2592.44	2574.89

IV. CONCLUSIONS

We have conducted a thorough test on the molecular probability of the $X(3872)$ in the $D^0\bar{D}^{*0}$ and D^+D^{*-} components. We do three exercises. First we start from a genuine, nonmolecular state, which however has to couple to the former components to be observable in these channels, as is the case experimentally. Then we force the state to produce a bound state at a certain energy. We show that the state gets unavoidably dressed with the meson-meson components, to the point that the molecular probability becomes exactly unity when the binding approaches the $D^0\bar{D}^{*0}$ threshold, with this channel acquiring most of the probability compared to the charged channel D^+D^{*-}, eventually acquiring all of it in the limit of zero binding. Yet, there is the issue of how fast this probability goes to unity and we study this issue as a function of the bare mass of the genuine state prior to its dressing with the meson-meson components. We observe then that if the bare mass of the genuine state is very close to threshold, the raise of the molecular probability to unity occurs at even smaller distances to this threshold, to the point that for the experimental mass of the $X(3872)$ state, the molecular probability can be very small and we would have essentially a nonmolecular state. This is the first conclusion of the paper, that the binding energy by itself does not determine the nature of the $X(3872)$ state. Yet, in this case we also observe that the scattering length of the $D^0\bar{D}^{*0}$ channel becomes very small and the effective range grows up to values bigger than 500 fm, in flagrant disagreement with present experimental values. The different cases studied allow us to conclude that if one starts with a pure genuine state, without consideration of any direct interaction of the meson-meson components and we force it to be responsible for the binding of the $X(3872)$ state, the state becomes essentially pure molecular at the end. We definitely rule out this scenario.

The next test consists in including a direct interaction between the meson-meson components. This interaction exists and is calculated by many groups independently. We take a reasonable interaction provided by vector exchange, but scaled such that by itself does not produce binding of the meson-meson components. What we observe is that,

as soon as a reasonable direct meson-meson interaction is considered, the molecular probability is drastically increased. We find however, that this kind of hybrid picture is not forbidden by present data of the scattering length and effective range, but even then the molecular probability is of the order of 95%.

Finally, we also conduct a test using a pure molecular picture in which there is no genuine state. In this case, by construction, the molecular probability is unity but we determine the values of the scattering length and effective range and see that, while certainly compatible with present experimental values, they differ appreciably from the hybrid scenario discussed above. We also point out the relevance of the scattering length and effective range for the D^+D^{*-} channel, that has not been given attention so far, neither theoretically nor experimentally, and conclude that a determination of these magnitudes together with more precise values of a and r_0 for the $D^0\bar{D}^{*0}$ channel will be extremely useful in the future to further pin down the molecular probability of the $X(3872)$. While with present data we can certainly rule out a picture in which the nonmolecular component of the $X(3872)$ is dominant, the precise value of the molecular components will have to wait for more precise measurements of the scattering length and effective range for the $D^0\bar{D}^{*0}$ and D^+D^{*-} channels.

ACKNOWLEDGMENTS

This work is partly supported by the National Natural Science Foundation of China under Grants No. 12175066, No. 11975009, and No. 12247108 and the China Postdoctoral Science Foundation under Grant No. 2022M720359. This work is also partly supported by the Spanish Ministerio de Economia y Competitividad (MINECO) and European FEDER funds under Contracts No. FIS2017-84038-C2-1-P B and No. PID2020–112777GB-I00, and by Generalitat Valenciana under Contract No. PROMETEO/2020/023. This project has received funding from the European Union Horizon 2020 research and innovation programme under the program H2020-INFRAIA-2018-1, Grant Agreement No. 824093 of the STRONG-2020 project. This research is also supported by the Munich Institute for Astro-, Particle and BioPhysics (MIAPbP) which is funded by the Deutsche Forschungsgemeinschaft (DFG, German Research Foundation) under Germany's Excellence Strategy-EXC-2094-390783311.

[1] A. Esposito, A. L. Guerrieri, F. Piccinini, A. Pilloni, and A. D. Polosa, Int. J. Mod. Phys. A **30**, 1530002 (2015).
[2] R. F. Lebed, R. E. Mitchell, and E. S. Swanson, Prog. Part. Nucl. Phys. **93**, 143 (2017).
[3] H.-X. Chen, W. Chen, X. Liu, and S.-L. Zhu, Phys. Rep. **639**, 1 (2016).
[4] F.-K. Guo, C. Hanhart, U.-G. Meißner, Q. Wang, Q. Zhao, and B.-S. Zou, Rev. Mod. Phys. **90**, 015004 (2018); **94**, 029901(E) (2022).
[5] Y. S. Kalashnikova and A. V. Nefediev, Phys. Usp. **62**, 568 (2019).
[6] Y. Yamaguchi, A. Hosaka, S. Takeuchi, and M. Takizawa, J. Phys. G **47**, 053001 (2020).
[7] N. Brambilla, S. Eidelman, C. Hanhart, A. Nefediev, C.-P. Shen, C. E. Thomas, A. Vairo, and C.-Z. Yuan, Phys. Rep. **873**, 1 (2020).
[8] F.-K. Guo, X.-H. Liu, and S. Sakai, Prog. Part. Nucl. Phys. **112**, 103757 (2020).
[9] H.-X. Chen, W. Chen, X. Liu, Y.-R. Liu, and S.-L. Zhu, Rep. Prog. Phys. **86**, 026201 (2023).
[10] M. Mai, U.-G. Meißner, and C. Urbach, Phys. Rep. **1001**, 1 (2023).
[11] E. Braaten, L.-P. He, and J. Jiang, Phys. Rev. D **103**, 036014 (2021).
[12] M.-Z. Liu and L.-S. Geng, Eur. Phys. J. C **81**, 179 (2021).
[13] L. Meng, B. Wang, and S.-L. Zhu, Sci. Bull. **66**, 1288 (2021).
[14] X.-K. Dong, F.-K. Guo, and B.-S. Zou, Prog. Phys. **41**, 65 (2021).
[15] Q. Wu, D.-Y. Chen, and T. Matsuki, Eur. Phys. J. C **81**, 193 (2021).
[16] M. C. Gordillo, F. De Soto, and J. Segovia, Phys. Rev. D **104**, 054036 (2021).
[17] X.-K. Dong, F.-K. Guo, and B.-S. Zou, Commun. Theor. Phys. **73**, 125201 (2021).
[18] L. Meng, G.-J. Wang, B. Wang, and S.-L. Zhu, Phys. Rev. D **104**, 094003 (2021).
[19] Y. Kamiya, T. Hyodo, and A. Ohnishi, Eur. Phys. J. A **58**, 131 (2022).
[20] Z.-Y. Lin, J.-B. Cheng, and S.-L. Zhu, arXiv:2205.14628.
[21] T. Ji, X.-K. Dong, M. Albaladejo, M.-L. Du, F.-K. Guo, and J. Nieves, Phys. Rev. D **106**, 094002 (2022).
[22] Y. Wang, Q. Wu, G. Li, W.-H. Qin, X.-H. Liu, C.-S. An, and J.-J. Xie, Phys. Rev. D **106**, 074015 (2022).
[23] H.-N. Wang, L.-S. Geng, Q. Wang, and J.-J. Xie, Chin. Phys. Lett. **40**, 021301 (2023).
[24] T. Kinugawa and T. Hyodo, arXiv:2303.07038.
[25] G. Yang, J. Ping, and J. Segovia, Eur. Phys. J. C **83**, 772 (2023).
[26] Q. Wu, M.-Z. Liu, and L.-S. Geng, arXiv:2304.05269.
[27] F.-Z. Peng, M.-J. Yan, and M. Pavon Valderrama, arXiv:2304.13515.
[28] I. Terashima and T. Hyodo, Phys. Rev. C **108**, 035204 (2023).

[29] P.-P. Shi, F. Huang, and W.-L. Wang, Phys. Rev. D **103**, 094038 (2021).
[30] A. Esposito, L. Maiani, A. Pilloni, A. D. Polosa, and V. Riquer, Phys. Rev. D **105**, L031503 (2022).
[31] H. X. Huang, X. Jin, Y. Tan, and J. L. Ping, Europhys. Lett. **135**, 31001 (2021).
[32] C. Chen, H. Chen, W.-Q. Niu, and H.-Q. Zheng, Eur. Phys. J. C **83**, 52 (2023).
[33] A. Sharma and A. Upadhyay, Phys. Scr. **98**, 095308 (2023).
[34] R. F. Lebed and S. R. Martinez, Phys. Rev. D **106**, 074007 (2022).
[35] G.-J. Wang, Z. Yang, J.-J. Wu, M. Oka, and S.-L. Zhu, arXiv:2306.12406.
[36] X.-W. Kang and J. A. Oller, Eur. Phys. J. C **77**, 399 (2017).
[37] V. Baru, C. Hanhart, Y. S. Kalashnikova, A. E. Kudryavtsev, and A. V. Nefediev, Eur. Phys. J. A **44**, 93 (2010).
[38] H. Zhang, J. Liao, E. Wang, Q. Wang, and H. Xing, Phys. Rev. Lett. **126**, 012301 (2021).
[39] B. Wu, X. Du, M. Sibila, and R. Rapp, Eur. Phys. J. A **57**, 122 (2021); **57**, 314(E) (2021).
[40] E. Braaten, L.-P. He, K. Ingles, and J. Jiang, Phys. Rev. D **103**, L071901 (2021).
[41] H.-G. Xu, Z.-L. She, D.-M. Zhou, L. Zheng, X.-L. Kang, G. Chen, and B.-H. Sa, Eur. Phys. J. C **81**, 784 (2021).
[42] M. Albaladejo, J. M. Nieves, and L. Tolos, Phys. Rev. C **104**, 035203 (2021).
[43] L. R. Dai, J. Song, and E. Oset, Phys. Lett. B **846**, 138200 (2023).
[44] R. L. Workman *et al.* (Particle Data Group), Prog. Theor. Exp. Phys. **2022**, 083C01 (2022).
[45] R. Molina, D. Nicmorus, and E. Oset, Phys. Rev. D **78**, 114018 (2008).
[46] L. S. Geng and E. Oset, Phys. Rev. D **79**, 074009 (2009).
[47] R. Molina and E. Oset, Phys. Lett. B **811**, 135870 (2020).
[48] D. Gamermann, J. Nieves, E. Oset, and E. Ruiz Arriola, Phys. Rev. D **81**, 014029 (2010).
[49] D. Gamermann and E. Oset, Phys. Rev. D **80**, 014003 (2009).
[50] T. Hyodo, Int. J. Mod. Phys. A **28**, 1330045 (2013).
[51] M. Bando, T. Kugo, and K. Yamawaki, Phys. Rep. **164**, 217 (1988).
[52] M. Harada and K. Yamawaki, Phys. Rep. **381**, 1 (2003).
[53] U. G. Meissner, Phys. Rep. **161**, 213 (1988).
[54] H. Nagahiro, L. Roca, A. Hosaka, and E. Oset, Phys. Rev. D **79**, 014015 (2009).
[55] N. Ikeno, R. Molina, and E. Oset, Phys. Lett. B **814**, 136120 (2021).
[56] J. M. Dias, G. Toledo, L. Roca, and E. Oset, Phys. Rev. D **103**, 116019 (2021).
[57] M. C. Birse, Z. Phys. A **355**, 231 (1996).
[58] L. R. Dai, L. M. Abreu, A. Feijoo, and E. Oset, Eur. Phys. J. C **83**, 983 (2023).
[59] R. Aaij *et al.* (LHCb Collaboration), Phys. Rev. D **102**, 092005 (2020).
[60] V. Baru, X.-K. Dong, M.-L. Du, A. Filin, F.-K. Guo, C. Hanhart, A. Nefediev, J. Nieves, and Q. Wang, Phys. Lett. B **833**, 137290 (2022).
[61] V. Baru (private communication).
[62] A. Feijoo, W. H. Liang, and E. Oset, Phys. Rev. D **104**, 114015 (2021).
[63] R. Aaij *et al.* (LHCb Collaboration), Nat. Commun. **13**, 3351 (2022).
[64] M. Mikhasenko, arXiv:2203.04622.
[65] Mishados (private communication).
[66] M. Albaladejo and J. Nieves, Eur. Phys. J. C **82**, 724 (2022).
[67] J. Song, L. R. Dai, and E. Oset, Eur. Phys. J. A **58**, 133 (2022).
[68] S. Weinberg, Phys. Rev. **137**, B672 (1965).